ARTICLE
Journal of Cellular Biochemistry 108:935–946 (2009)

Journal of Cellular Biochemistry

Proteasome Inhibition Activates the Mitochondrial Pathway of Apoptosis in Human CD4$^+$ T Cells

Carsten Berges, Heinrich Haberstock, Dominik Fuchs, Mahmoud Sadeghi, Gerhard Opelz, Volker Daniel, and Cord Naujokat*

Department of Transplantation Immunology, Institute of Immunology, University of Heidelberg, Im Neuenheimer Feld 305, D-69120 Heidelberg, Germany

ABSTRACT

We have previously shown that inhibition of the proteolytic activity of the proteasome induces apoptosis and suppresses essential functions of activated human CD4$^+$ T cells, and we report now the detailed mechanisms of apoptosis following proteasome inhibition in these cells. Here we show that proteasome inhibition by bortezomib activates the mitochondrial pathway of apoptosis in activated CD4$^+$ T cells by disrupting the equilibrium of pro-apoptotic and anti-apoptotic proteins at the outer mitochondrial membrane (OMM) and by inducing the generation of reactive oxygen species (ROS). Proteasome inhibition leads to accumulation of pro-apoptotic proteins PUMA, Noxa, Bim and p53 at the OMM. This event provokes mitochondrial translocation of activated Bax and Bak homodimers, which induce loss of mitochondrial membrane potential ($\Delta\Psi$m). Breakdown of $\Delta\Psi$m is followed by rapid release of pro-apoptotic Smac/DIABLO and HtrA2 from mitochondria, whereas release of cytochrome *c* and AIF is delayed. Cytoplasmic Smac/DIABLO and HtrA2 antagonize IAP-mediated inhibition of partially activated caspases, leading to premature activation of caspase-3 followed by activation of caspase-9. Our data show that proteasome inhibition triggers the mitochondrial pathway of apoptosis by activating mutually independent apoptotic pathways. These results provide novel insights into the mechanisms of apoptosis induced by proteasome inhibition in activated T cells and underscore the future use of proteasome inhibitors for immunosuppression. J. Cell. Biochem. 108: 935–946, 2009.

KEY WORDS: T CELLS; PROTEASOME; PROTEASOME INHIBITION; BORTEZOMIB; MITOCHONDRIAL APOPTOTIC PATHWAY

The 26S proteasome constitutes the central proteolytic unit of the ubiquitin-proteasome-system (UPS) and plays a key role in the regulation and perpetuation of basic cellular functions by processing cell proteins essential for differentiation, proliferation, cell cycling, apoptosis, gene transcription, signal transduction, senescence, inflammatory response and immune activation [Glickman and Ciechanover, 2002; Naujokat and Hoffmann, 2002; Ciechanover, 2006].

Synthetic and microbial proteasome inhibitors have contributed to the identification of multiple functions of the 26S proteasome in various processes and pathways of eukaryotic cells [Naujokat and Hoffmann, 2002; Groll and Huber, 2004; Naujokat et al., 2007b]. It has been demonstrated that inhibition of proteolytic proteasome activity induces apoptosis preferentially in proliferating and neoplastic cells [Drexler, 1997; Naujokat et al., 2000; Naujokat and Hoffmann, 2002]. Proteasome inhibitors like bortezomib have been shown to be effective in the treatment of diverse cancers, including multiple myeloma, non-Hodgkin's lymphoma, acute leukemias and prostate cancer [Orlowski and Kuhn, 2008]. Several studies have demonstrated an efficacy of proteasome inhibitors in the treatment of deregulated T cell-mediated immune responses that contribute to the pathogenesis of polyarthritis, psoriasis, lupus erythematosus, allograft rejection and graft-versus-host disease (GVHD) [Luo et al., 2001; Mattingly et al., 2007; Everly et al., 2008;

Abbreviations used: DC, dendritic cells; OMM, outer mitochondrial membrane; MOMP, mitochondrial outer membrane permeabilization; ROS, reactive oxygen species; $\Delta\Psi$m, mitochondrial membrane potential; UPS, ubiquitin-proteasome-system; GVHD, graft-versus-host disease; BioALVS, AdaK(Bio)AhX3L3VS; Bor, bortezomib; RIPA, radio immunoprecipitation assay; ZVAD, *N*-benzyloxycarbonyl-valyl-alanyl-aspartyl-fluoromethylketone; bioVAD, biotinylated-*N*-benzyloxycarbonyl-valyl-alanyl-aspartyl-fluoromethylketone; DCF, 6-carboxy-2′,7′-dichlorodihydrofluorescein; NAC, *N*-acetylcysteine; ECL, enhanced chemiluminescence; PVDF, polyvinylidene fluoride; SDS, sodium-dodecyl sulphate polyacrylamide.

Carsten Berges and Heinrich Haberstock contributed equally to this work.

*Correspondence to: Dr. Cord Naujokat, Department of Transplantation Immunology, Institute of Immunology, University of Heidelberg, Im Neuenheimer Feld 305, D-69120 Heidelberg, Germany.
E-mail: cord.naujokat@med.uni-heidelberg

Received 20 March 2009; Accepted 28 July 2009 • DOI 10.1002/jcb.22325 • © 2009 Wiley-Liss, Inc.
Published online 4 September 2009 in Wiley InterScience (www.interscience.wiley.com).

Neubert et al., 2008; Perry et al., 2008]. We and others have previously shown that inhibition of the proteolytic activity of the 26S proteasome interfere with essential immune functions of human dendritic cells (DC) and activated T cells, suggesting that proteasome inhibitors can potentially be used as immunosuppressive agents [Blanco et al., 2006; Naujokat et al., 2007b; Berges et al., 2008].

Induction of apoptosis is one candidate mechanism for the suppression of T cell-mediated immune responses by proteasome inhibition, and it has been shown that activated T cells are preferentially susceptible to proteasome inhibition [Blanco et al., 2006; Berges et al., 2008].

Numerous studies in neoplastic cells indicate that multiple mechanisms are responsible for induction of apoptosis by proteasome inhibition, including receptor-mediated and mitochondrial apoptotic pathways [Chauhan et al., 2005]. On the other hand, proteasome inhibition may preferentially activate certain apoptotic mechanisms dependent on the cell type and the differentiation state of the particular cell. Several studies describe cellular mechanisms that confer resistance to proteasome inhibition in vitro and in vivo [Naujokat et al., 2007b; Orlowski and Kuhn, 2008; Fuchs et al., 2008a,b]. Thus, in spite of preclinical results obtained with proteasome inhibitors in the treatment of GVHD, allograft rejection and immune disorders [Luo et al., 2001; Sun et al., 2004; Mattingly et al., 2007; Everly et al., 2008; Neubert et al., 2008; Perry et al., 2008], the mechanisms of apoptosis induction by these compounds is still poorly understood.

Aiming at the clinical use of proteasome inhibitors, especially as immunosuppressive agents, it is important to decipher the particular apoptotic pathways in a specific and relevant cell type. Here we report the detailed mechanisms of apoptosis induced by proteasome inhibition in human $CD4^+$ T cells activated in a physiological manner by allogeneic DCs. We demonstrate that proteasome inhibition activates the mitochondrial pathway of apoptosis in activated T cells by disrupting the equilibrium of pro- and anti-apoptotic proteins at the outer mitochondrial membrane (OMM) and by generating reactive oxygen species (ROS).

MATERIALS AND METHODS

ANTIBODIES AND REAGENTS

Bortezomib was provided by Janssen-Cilag (Neuss, Germany). Human recombinant (rh) granulocyte macrophage colony-stimulating factor (GM-CSF), rh Interleukin-4 (IL-4), rh Interferon-γ (IFN-γ) were all purchased from AL-Immunotools (Friesoythe, Germany). LPS from *Escherichia coli* 055:B5, *N*-acetylcysteine (NAC) was obtained from Sigma (Heidelberg, Germany). The non-biotinylated pan caspase-inhibitor *N*-benzyloxycarbonyl-valyl-alanyl-aspartyl-fluoromethylketone (ZVAD) was purchased from Bachem (Weil am Rhein, Germany), the biotinylated-VAD (bioVAD) was obtained from MP Germany (Heidelberg, Germany). Dye 6-carboxy-2′,7′-dichlorodihydrofluorescein (DCF) was obtained from Molecular Probes/Invitrogen (Karlsruhe, Germany).

Primary monoclonal and polyclonal (mAb, pAb) antibodies were obtained from the following sources: anti-AIF (E-1, mouse mAb), anti-Bak (G-23, rabbit pAb), anti-Bax (N-20, rabbit pAb), anti-Bcl-2 (N-19, rabbit pAb), anti-Bcl-XS/L (S-18, rabbit pAb), anti-Bid (FL-195, rabbit pAb), anti-Bim (H-191, rabbit pAb), anti-caspase-8 (90A992, mouse mAb), anti-cIAP1 (H-83, rabbit pAb), anti-cIAP2 (H-85, rabbit pAb), anti-cytochrome c (7H8, mouse mAb), anti-$cFLIP_{S/L}$ (G-11, mouse mAb), anti-HtrA2 (1B3, mouse mAb), anti-ICAD (FL-331, rabbit pAb), anti-Mcl-1 (22, mouse mAb), anti-Noxa (114C307, mouse mAb), anti-p53 (DO-1, mouse mAb), anti-PARP (H-250, rabbit pAb), anti-PUMA α/β (FL-193, rabbit pAb), anti-Smac/DIABLO (FL-239, rabbit pAb) and anti-XIAP (A-7, mouse mAb): Santa Cruz (Heidelberg, Germany); anti-caspase-3 (rabbit pAb), anti-caspase-9 (rabbit pAb), anti-caspase-9p10 (F-7; mouse mAb) and anti-COX IV (rabbit pAb): Cell Signaling (Frankfurt, Germany); anti-mono- and poly-ubiqutininylated proteins (clone FK2, mouse mAb): Biomol (Hamburg, Germany); anti-β-actin (AC-15, mouse mAb): Sigma. Secondary horseradish peroxidase-conjugated (HRP) anti-rabbit and anti-mouse antibodies were obtained from Pierce (Bonn, Germany).

GENERATION OF DCS

DCs were generated from human healthy donor $CD14^+$ monocytes isolated from heparinized peripheral blood by Ficoll (Innotrain, Kronberg, Germany) density gradient centrifugation and subsequent negative isolation with immunomagnetic beads (Dynal/Invitrogen, Karlsruhe, Germany). DCs were generated as described previously [Naujokat et al., 2007a].

T CELL PURIFICATION AND ACTIVATION

$CD4^+$ T cells were isolated and activated as described before [Berges et al., 2008]. Freshly isolated $CD4^+$ T cells were considered as non-activated resting T cells.

ANALYSIS OF APOPTOSIS

Apoptotic cell death was determined using the Annexin V-FITC/PI kit from BD biosciences. Briefly, activated $CD4^+$ T cells or U266 B cells were pretreated for 1 h with 100 μM ZVAD or 1 mM NAC, or left untreated followed by 24 h treatment with 10 nM bortezomib. Cells were subsequently harvested and stained with Annexin V-FITC and PI for 15 min at room temperature (RT) in the dark. Apoptosis of cells was measured and quantified using a FACScan flow cytometer and Cellquest software (BD Pharmingen, Heidelberg). Percentages of specific apoptosis were calculated as described previously [Dhein et al., 1997] using the following formula:

$$SA\,(\%) = 100 \times \frac{A_E - A_C}{100 - A_C}$$

where AE equals % of apoptotic cells in the experimental group, and AC equals % of apoptotic cells in the control group.

ANALYSIS OF MITOCHONDRIAL DEPOLARIZATION

5,5′,6,6-Tetrachloro-1,1′,3,3′-tetraethyl-benzimidazolylcarbocyanine (JC-1) (Sigma) was employed to measure mitochondrial depolarization in activated $CD4^+$ T cells and U266 B cells. Cells (2×10^5) were preincubated with 1 mM NAC and 100 μM ZVAD for 1 h, followed by incubation with bortezomib or DMSO for 6 and 24 h. Cells were subsequently harvested and resuspended in fresh

CM with pre-warmed 10% FCS. Cells were stained for 20 min with 2,5 μg/ml JC-1 at RT in the dark. After washing twice in PBS, $\Delta\Psi m$ was determined by flow cytometry.

DETECTION OF INTRACELLULAR PEROXIDES AND SUPEROXIDE

Measurements of intracellular ROS were performed by using cell-permeable dyes as described previously [Miller et al., 2007].

PREPARATION OF CELL LYSATES AND IMMUNOBLOTTING

For isolation of whole cell lysates (WCL), cells were treated for the indicated time with bortezomib or DMSO control. Activated and resting $CD4^+$ T cells were subsequently lysed for 30 min in cold radio immunoprecipitation assay (RIPA) buffer. Homogenates were centrifuged at 10,000*g* for 10 min at 4°C, and the supernatant was used for further analysis. For analysis of release of intramitochondrial proteins into the cytoplasm, mitochondrial and cytoplasmic proteins were obtained as described previously [Nencioni et al., 2005]. Briefly, 5×10^6 cells were resuspended in 100 μl of cold 0.025% digitonin (Sigma) in a lysis buffer (250 mM sucrose, 20 mM Hepes [*N*-2-hydroxyethylpiperazine-*N*′-2-ethanesulfonic acid, pH 7.4], 5 mM $MgCl_2$, 10 mM KCl, 1 mM EDTA [ethylenediaminetetraacetic acid], 1 tablet Complete Mini protease inhibitor (Roche, Penzberg)). After incubation on ice for 10 min, cells were centrifuged at 10,000*g* for 2 min, the supernatant was removed and considered as cytoplasmic fraction. The remaining pellet was resuspended in 100 μl of cold 2% CHAPS (Sigma) in a lysis buffer (25 mM Tris/HCl (pH 7.2) 150 mM NaCl) by vortexing for 1 min. Subsequently, cells were centrifuged for 2 min at 10,000*g* and the supernatant was removed and considered as mitochondrial fraction. Equal amounts of protein were separated by sodium-dodecyl sulphate–polyacrylamide (SDS–PAGE) and electrotransferred onto polyvinylidene fluoride (PVDF) membranes. After blocking, the membranes were probed with primary antibodies followed by HRP-conjugated secondary antibodies. Immunoreactive bands were visualized by enhanced chemiluminescence (ECL) using Supersignal West Femto Chemiluminescence Reagent (Pierce).

PROBING PROTEASOME β-SUBUNIT ACTIVITY

Affinity labeling of active proteasome subunits using the proteasome specific affinity probe BioALVS was performed as described previously [Berges et al., 2008]. Briefly, activated T cells were incubated with the indicated amounts of each inhibitor for 1 h. The cells were washed two times and pelleted with ice-cold PBS. A volume of glass beads (<106 μm, acid washed, Sigma) equivalent to the volume of the pellet was added, followed by a similar volume of homogenization buffer (50 mM Tris pH 7.4, 1 mM DTT, 5 mM $MgCl_2$, 2 mM ATP, 250 mM sucrose). Cells were vortexed at high speed for 1 min, and the beads and cell debris were removed by centrifugation at 10,000*g* for 5 min at 4°C. The resulting supernatant was centrifuged at 10,000*g* for 20 min at 4°C to remove intact cells and nuclei. Protein concentration was determined using DC-Protein assay (Bio-Rad, Munich, Germany). Equal amounts of cell lysates (approximately 25 μg) were incubated with 4 μg of BioALVS for 2 h at 37°C. Subsequently, proteins were denatured by boiling in reducing 4X sample buffer, separated on 12% SDS–PAGE Tris–HCl Gels and electrotransferred onto PVDF membranes. Immunoblotting was performed using Vectastain (Vector-Laboratories, Burlingame, England) followed by ECL (Pierce, Bonn, Germany).

CASPASE PRECIPITATION ASSAY

Caspase activity precipitation assays were performed according to a previously described protocol [Misra et al., 2005]. Briefly, activated, bortezomib or DMSO treated $CD4^+$ T cells were incubated with 20 μM bioVAD at 37°C for 1 h. As negative control, a portion of $CD4^+$ T cells was incubated with 100 μM ZVAD prior to incubation with bioVAD. Cells were lysed in RIPA buffer containing 20 μM bioVAD. Six hundred micrograms of lysate was precleared by rocking with 40 μl of Sepharose 6B-agarose beads (Sigma) at 4°C for 1 h. Supernatants were then rocked with 60 μl of streptavidin-Sepharose beads (Zymed-Invitrogen) at 4°C overnight. Beads were washed 5 times in RIPA buffer without protease inhibitor and then boiled in loading buffer. Beads were removed by centrifugation, and immunoblot analysis of precipitates was performed with specific caspase antibodies to identify active caspases. WCL (input) were included to positively identify each caspase band and assess their overall expression.

STATISTICAL ANALYSES

Statistical analysis was performed using Excel software. Differences between mean values were assessed using two-tailed paired Student's *t*-test. Statistical significance was set at $P < 0.05$.

RESULTS

PROTEASOME INHIBITION BY BORTEZOMIB IN ACTIVATED $CD4^+$ T CELLS

The inhibitory profile of bortezomib towards proteasomal proteolytic subunits was investigated in activated $CD4^+$ T cells by affinity labeling using the proteasome-specific affinity probe AdaK-(Bio)AhX3L3VS (BioALVS). We have previously shown that $CD4^+$ T cells activated with allogeneic DCs express all of the proteasomal proteolytic subunits β1, β1i, β2, β2i, β5 and β5i [Berges et al., 2008]. Affinity labeling using BioALVS, which targets these proteolytic subunits, reveals that bortezomib at 10 nM occupies and inhibits primarily β1, β1i, β5 and β5i subunits (Fig. 1A). To demonstrate proteasome inhibition in functional terms, we performed immunoblot analysis of polyubiquitinated proteins in activated $CD4^+$ T cells exposed to 10 nM bortezomib (Fig. 1B).

PROTEASOME INHIBITION INDUCES FURTHER PROCESSING OF CASPASE-3 AND -9

We have previously shown that inhibition of the proteolytic activities of the 26S proteasome by bortezomib induces apoptosis in activated $CD4^+$ T cells [Berges et al., 2008]. To elucidate the pathway of apoptosis induced by proteasome inhibition in activated $CD4^+$ T cells, we analyzed the processing degree of caspase-8, which initiates receptor-mediated apoptosis, of caspase-9, the initiator of mitochondria-mediated apoptosis, and of caspase-3, the most relevant effector caspase. As shown earlier by others [Misra et al., 2005; Lamkanfi et al., 2007], activated T cells exhibit partially processed caspases, and we could confirm these results (1C). In particular, activated T cells expressed procaspase-8 as well as

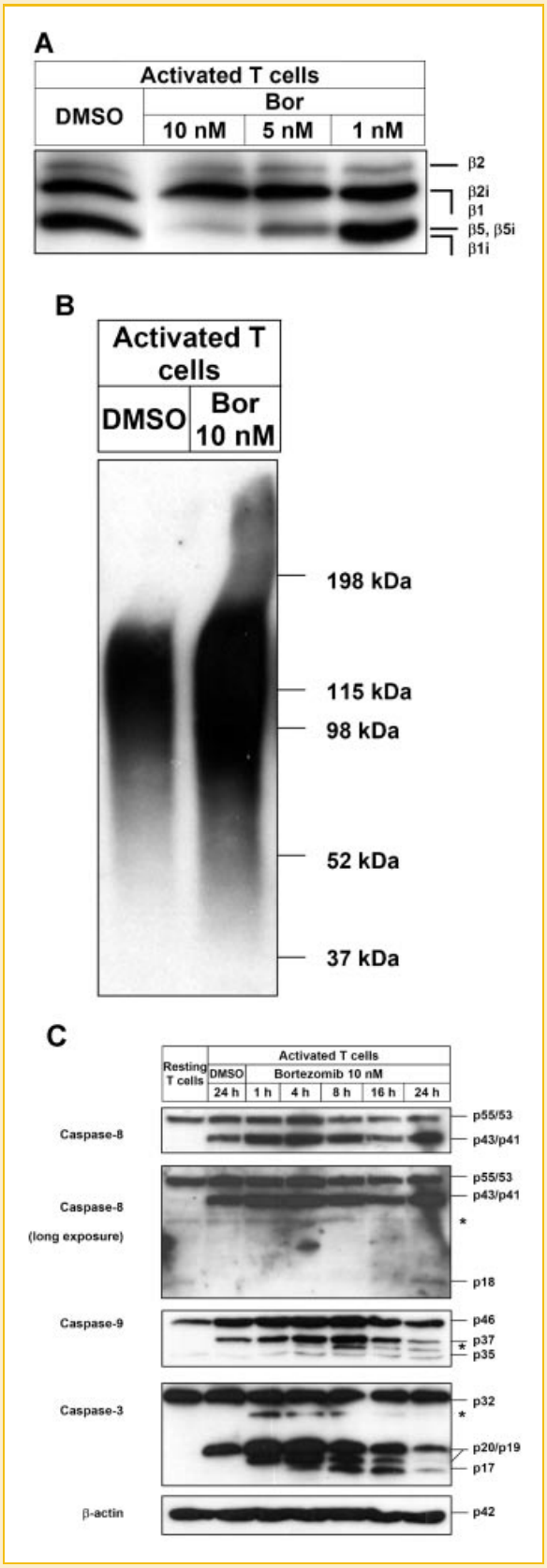

p43/p41 caspase-8. Proteasome inhibition by apoptosis-inducing concentrations of bortezomib [Berges et al., 2008] did not considerably change the processing pattern of caspase-8. Of note, the presence of fully proteolytic active caspase-8p18 fragment after exposure to bortezomib for 24 h was only detectable at longer film exposure (Fig. 1C). Activated $CD4^+$ T cells mainly displayed expression of unprocessed procaspase-9. Caspase-9p37 fragment, which is generated by proteolytic active caspase-3, was also detected (Fig. 1C). Proteasome inhibition induced a rapid increase of caspase-9p37 fragment and induction of caspase-9p35 fragment that is created by autoprocessing of procaspase-9 (Fig. 1C). Caspase-3 was detected as both unprocessed procaspase-3 and processed caspase-3p20 fragment (Fig. 1C), the latter is known to be slightly proteolytic active [Sun et al., 2002]. Proteasome inhibition induced a further processing of caspase-3 to proteolytic active caspase-3p19 and to fully mature caspase-3p17 fragment. By contrast, resting $CD4^+$ T cells only expressed unprocessed proforms of caspase-3, -8, and -9.

PROTEASOME INHIBITION INDUCES AN INCREASE IN CLEAVAGE OF CHARACTERISTIC CASPASE PROTEIN SUBSTRATES

Figure 2 shows that known caspase substrates like c-FLIP, PARP, and ICAD are partially cleaved in activated $CD4^+$ T cells. Proteasome inhibition induced a time-dependent accumulation of the c-FLIP splice variants c-$FLIP_L$ and c-$FLIP_S$ and the cleavage variant p43FLIP. In addition, appearance of the c-FLIP cleavage variant p22FLIP and of c-$FLIP_R$, another c-FLIP splice form [Krammer et al., 2007], was observed. Proteasome inhibition induced a slight accumulation of uncleaved Bid. The known caspase-3 substrates PARP and ICAD are already partially cleaved in activated $CD4^+$ T cells. By contrast, resting $CD4^+$ T cells displayed expression of only full-length PARP and both ICAD-splice forms. Proteasome

Fig. 1. Proteasome inhibition by bortezomib and induction of further processing of already processed caspases in activated $CD4^+$ T cells. A: affinity labeling of active proteasome subunits in activated $CD4^+$ T cells using the proteasome specific affinity probe BioALVS after incubation of cells with different concentrations of Bor for 1 h. B: Immunoblot analysis of accumulation of polyubiquitinated proteins in activated $CD4^+$ T cells using the FK2 monoclonal antibody which detects mono- and polyubiquitinated proteins. Purified $CD4^+$ T cells were activated for 4 days with allogeneic mDCs. Activated $CD4^+$ T cells were exposed for 24 h to DMSO or 10 nM Bor. C: immunoblot analysis of caspases-8, -9, and -3 expression. Purified $CD4^+$ T cells were left untreated (resting T cells) or were activated with allogeneic mDCs (activated T cells). Activated $CD4^+$ T cells were exposed for the indicated times to bortezomib (Bor) or for 24 h to DMSO. Cell lysates were prepared and analyzed for the expression of caspases-8, -9, and -3 by immunoblot. Caspase-8 represents non-cleaved procaspase-8, whereas caspase-8p43/41 bands represent fragments generated by cleavage at Asp374 or Asp384. A further cleavage at Asp216 produces caspase-8p18. Caspase-9 represents full-length protein, whereas caspase-9p37/p35 represent fragments generated by cleavage at Asp330 or Asp315. Caspase-3 represents noncleaved procaspase-3, caspase-3p20 represents a fragment generated by cleavage at Asp175, which is further autoprocessed to caspase-3p19/p17 at Asp9 or Asp28. Amounts of β-actin are shown as a control of equal protein loading. Immunoblots were performed in triplicate with similar results. Asterisks indicate nonspecific bands.

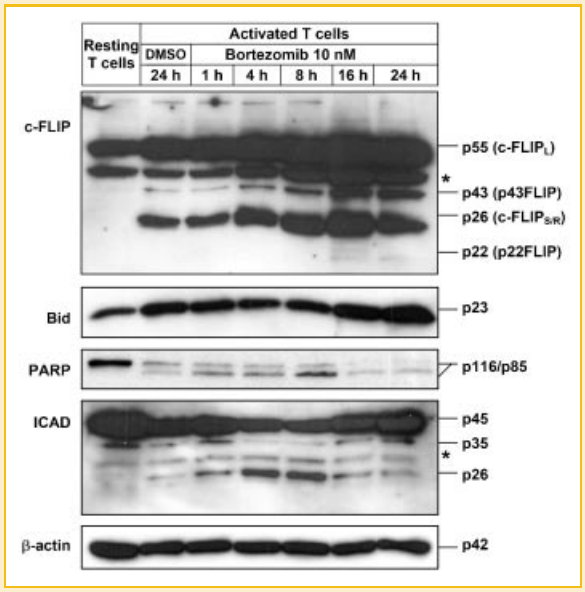

Fig. 2. Enhanced cleavage of caspase substrates in response to proteasome inhibition. Cell lysates were prepared from activated CD4$^+$ T cells and analyzed for the intracellular amounts of c-FLIP, Bid, PARP and ICAD by immunoblot. c-FLIP$_L$ represents full-length protein, p43FLIP and p22FLIP represent fragments generated by cleavage at Asp376 and Asp198, c-FLIP$_S$ and c-FLIP$_R$ represent noncleaved c-FLIP$_L$ splice variants. ICAD$_L$ and ICAD$_S$ are noncleaved ICAD splice variants, whereas ICADp26 corresponds to a cleavage product at Asp224. PARP represents full-length PARP and cleaved PARP (85 kDa) generated by cleavage at Asp211. Amounts of β-actin are shown as a control of equal protein loading. Caspase-8p12, which could be detected only with mouse monoclonal Ab clone 90A992, represents a fragment generated by further cleavage of caspase-8p43/41 at Asp216. Immunoblots were performed in triplicate with similar results. Asterisks indicate nonspecific bands.

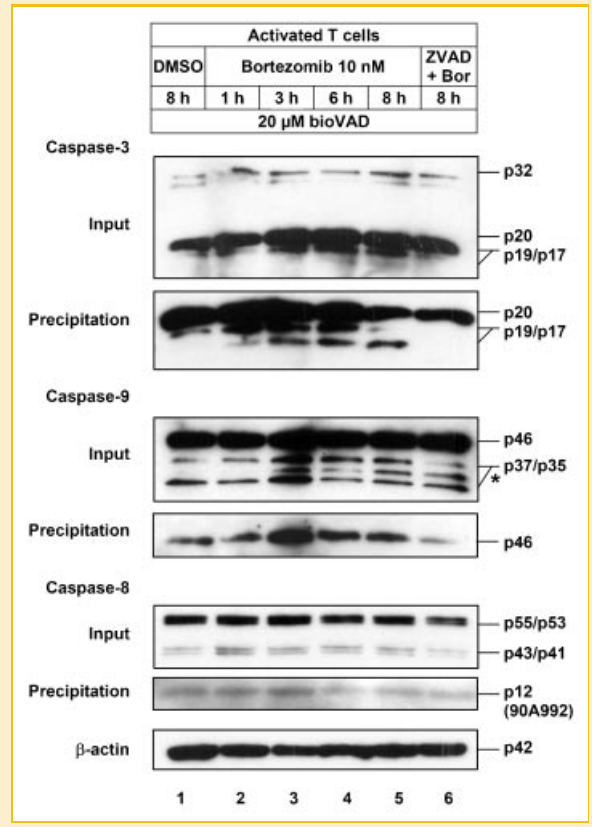

Fig. 3. Proteasome inhibition induces an increase in caspase-3 and -9 activity. A portion of cells was pretreated for 1 h with ZVAD followed by incubation with Bor for 8 h (lane 6). The rest of the cells were treated with Bor or DMSO as indicated. All cells were incubated with 20 μM bioVAD for another hour. Cells were lysed in buffer containing 20 μM bioVAD, and a portion of lysates were incubated with streptavidin-sepharose to reveal active caspases. Nonprecipitated lysates (input) were included in the analysis as a reference and to assess overall caspase expression. Immunoblot analysis was performed with precipitates and input for caspases-8, -9, and -3. Immunoblots were performed in triplicate with similar results. Asterisk indicates nonspecific bands.

inhibition induced a rapid enhancement of the 85 kDa PARP cleavage form and the ICAD cleavage product.

ENHANCEMENT OF CASPASE-3 AND -9 ACTIVITY IN RESPONSE TO PROTEASOME INHIBITION

In order to identify the particular caspase which is responsible for initiation of the apoptotic pathway induced by proteasome inhibition in activated CD4$^+$ T cells and because commercially available synthetic caspase peptide substrates and inhibitors lack selectivity [Berger et al., 2006], we performed caspase-activity precipitation assays according to a previously described protocol [Misra et al., 2005]. Activated CD4$^+$ T cells pretreated with bortezomib or DMSO were incubated with biotinylated ZVAD (bioVAD) which selectively binds enzymatically active caspase catalytic pockets. In agreement with our previous observations, caspase-3, -8, and -9 could be detected in a partially processed form in input samples of the cells (Fig. 3). Proteasome inhibition induced a rapid further processing of caspase-3 and -9, but not of caspase-8 (Fig. 3). Effector caspase-3 fragment p20 was precipitated, indicating that this fragment was enzymatically active. There was also negligible binding of bioVAD to caspase-3p19 (Fig. 3). Proteasome inhibition caused a rapid enhancement of caspase-3 activity within 1 h, as shown by an increase of caspase-3p19 fragment and the appearance of caspase-3p17, both precipitated by bioVAD (Fig. 3). A further increase in caspase-3 activity after proteasome inhibition was demonstrated by amplification of precipitated caspase-3p17. Caspase-9 was precipitated in its procaspase form (46 kDa). Proteasome inhibition leads to amplification of caspase-9 activity within 3 h, as shown by binding of more full-length caspase-9 to bioVAD (Fig. 3). In contrast to caspase-3 and -9, there was only slight binding of bioVAD to fully proteolytic active caspase-8p12 (Fig. 3). Proteasome inhibition failed to induce significant changes in caspase-8 activity. Pretreatment with ZVAD prior to bortezomib incubation competed for binding with bioVAD and, hence, decreased the amount of precipitated caspase-3, -9, and -8 (Fig. 3, lane 6).

DECREASED EXPRESSION OF IAPs IN RESPONSE TO PROTEASOME INHIBITION

To investigate whether pro-apoptotic caspase activity in the cells was blocked by pronounced expression of IAPs, which antagonize

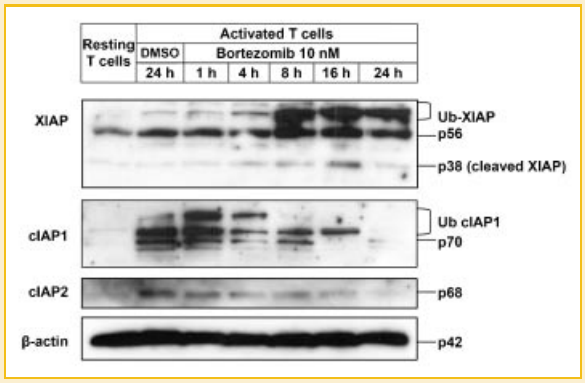

Fig. 4. Decreased expression of IAPs in response to proteasome inhibition. Cell lysates were prepared and analyzed for the intracellular amounts of XIAP, cIAP1 and cIAP2. XIAP and cIAP1 represent full-length proteins as well as ubiquitination and degradation products, whereas cIAP2 represents only full-length protein. Amounts of β-actin are shown as a control of equal protein loading. Immunoblots were performed in triplicate with similar results.

caspase activity [Vaux and Silke, 2005], and whether apoptosis induction caused relevant alterations in IAP abundance, we determined by immunoblot analysis the expression of principal IAP family members cIAP1, cIAP2 and XIAP in WCL of bortezomib-treated activated and resting $CD4^+$ T cells.

All IAPs analyzed were only weakly expressed in resting $CD4^+$ T cells (Fig. 4). Activated $CD4^+$ T cells showed a marked increase in XIAP, cIAP1 and cIAP2 expression, which is in accordance with the increase in caspase activity (Fig. 4). Beyond the expected XIAP and cIAP1 signals, we detected multiple higher and lower molecular mass forms characteristic of ubiquitination and degradation products. Proteasome inhibition induced a time-dependent accumulation of ubiquitinated and cleaved XIAP, whereas the abundance of XIAP was barely unchanged (Fig. 4). In contrast, we observed a gradual decrease of cIAP1 and cIAP2 and of all cIAP1 products.

PROTEASOME INHIBITION INDUCES RELEASE OF APOPTOGENIC INTRAMITOCHONDRIAL PROTEINS INTO THE CYTOPLASM

To test whether translocation of pro-apoptotic intramitochondrial proteins from mitochondria to the cytoplasm was responsible for the observed decrease in IAP abundance and the rapid increase in caspase-3 and -9 activity, we analyzed mitochondrial and cytoplasmic fractions of bortezomib-treated activated $CD4^+$ T cells for the presence of cytochrome *c*, Smac/DIABLO, HtrA2 and AIF. Proteasome inhibition induced a cytoplasmic translocation of cytochrome *c* and AIF after 16 h (Fig. 5A). We observed a rapid cytoplasmic translocation of Smac/DIABLO and HtrA2 after 4 and 8 h of bortezomib treatment, respectively. Hence, the release of these two pro-apoptotic proteins preceded the observed release of cytochrome *c* and AIF from mitochondria. To extent our analysis on other cells of the hematopoietic lineage, we performed the same experiments with mitochondrial and cytoplasmic fractions of bortezomib-treated U266 B cells. As shown in Figure 5B, all intramitochondrial pro-apoptotic proteins analyzed showed equal release from the mitochondria after 24 h of bortezomib treatment.

PROTEASOME INHIBITION INDUCES MOMP BY TRIGGERING TRANSLOCATION OF PRO-APOPTOTIC PROTEINS TO MITOCHONDRIA

In order to determine whether proteasome inhibition caused release of Smac/DIABLO, cytochrome *c*, HtrA2 and AIF by induction of MOMP, we analyzed cytoplasmic and mitochondrial fractions for the presence of pro- and anti-apoptotic members of the Bcl-2 family, which are known to regulate the mitochondrial pathway of apoptosis [Karst and Li, 2007]. We detected an increase in cytoplasmic abundance of Bid without detecting activated tBid (Fig. 6A). By contrast, PUMA, which is transcriptionally upregulated by p53 [Schuler and Green, 2001], was detected only in mitochondrial fractions, and proteasome inhibition induced a gradual accumulation of this pro-apoptotic BH3-only protein (Fig. 6A). Proteasome inhibition also led to an enrichment of all known Bim (Bim_{EL}, Bim_L, and Bim_S) splice variants and a dramatic increase of cytoplasmic and mitochondrial Noxa (Fig. 6A). Time-dependent accumulation of polyubiquitinated cytoplasmic p53 and non-ubiquitinated mitochondrial p53 could be detected after treatment of the cells with bortezomib. Proteasome inhibition induced an increase of the anti-apoptotic BH1-4 proteins Bcl-XL and Mcl-1 in cytoplasmic and in mitochondrial fractions. In contrast, abundance of anti-apoptotic Bcl-2, which is primarily localized to the mitochondrial membrane, showed a slight decrease in activated $CD4^+$ T cells as well as in U266 B cells (Figs. 6A and 5B). For the detection of Bax, we used the conformation-specific N20 antibody, which binds the activated form of Bax [Goping et al., 1998]. Figure 6B shows that proteasome inhibition induced a marked increase of cytoplasmic and mitochondrial Bax monomers and homodimers in activated $CD4^+$ T cells. We detected the BH123 effector protein Bak in both cytoplasmic and mitochondrial fractions of activated $CD4^+$ T cells. However, proteasome inhibition leads to the accumulation of cytoplasmic monomeric and mitochondrial homodimeric Bak.

PROTEASOME INHIBITION INDUCES LOSS OF MITOCHONDRIAL MEMBRANE POTENTIAL ($\Delta\Psi m$)

Activation and mitochondrial translocation of Bax and Bak is accompanied by the loss of mitochondrial membrane potential ($\Delta\Psi m$) [Wei et al., 2001]. To test whether bortezomib-induced translocation of activated Bax/Bak to the OMM results in the breakdown of $\Delta\Psi m$, which provokes subsequent release of pro-apoptotic proteins into the cytoplasm, we determined $\Delta\Psi m$ by flow cytometric measurement of red fluorescence after loading the cells with the cationic dye JC-1. Figure 6C demonstrates that proteasome inhibition induced a significant loss of $\Delta\Psi m$ after 6 and 24 h in activated $CD4^+$ T cells that could partly be reconstituted by preincubation of the cells with the unspecific ROS scavenger *N*-acetylcysteine (NAC) (Fig. 6C). This effect was not observed after pre-treatment of the cells with ZVAD, suggesting a prominent role for ROS generation in destruction of $\Delta\Psi m$ induced by proteasome inhibition. By contrast, pre-treatment of U266 B cells with ZVAD decreased bortezomib-induced loss of $\Delta\Psi m$ to a greater extent than NAC, indicating a more important role for caspase activity in destruction of $\Delta\Psi m$ induced by proteasome inhibition in U266 B cells (Fig. 6D).

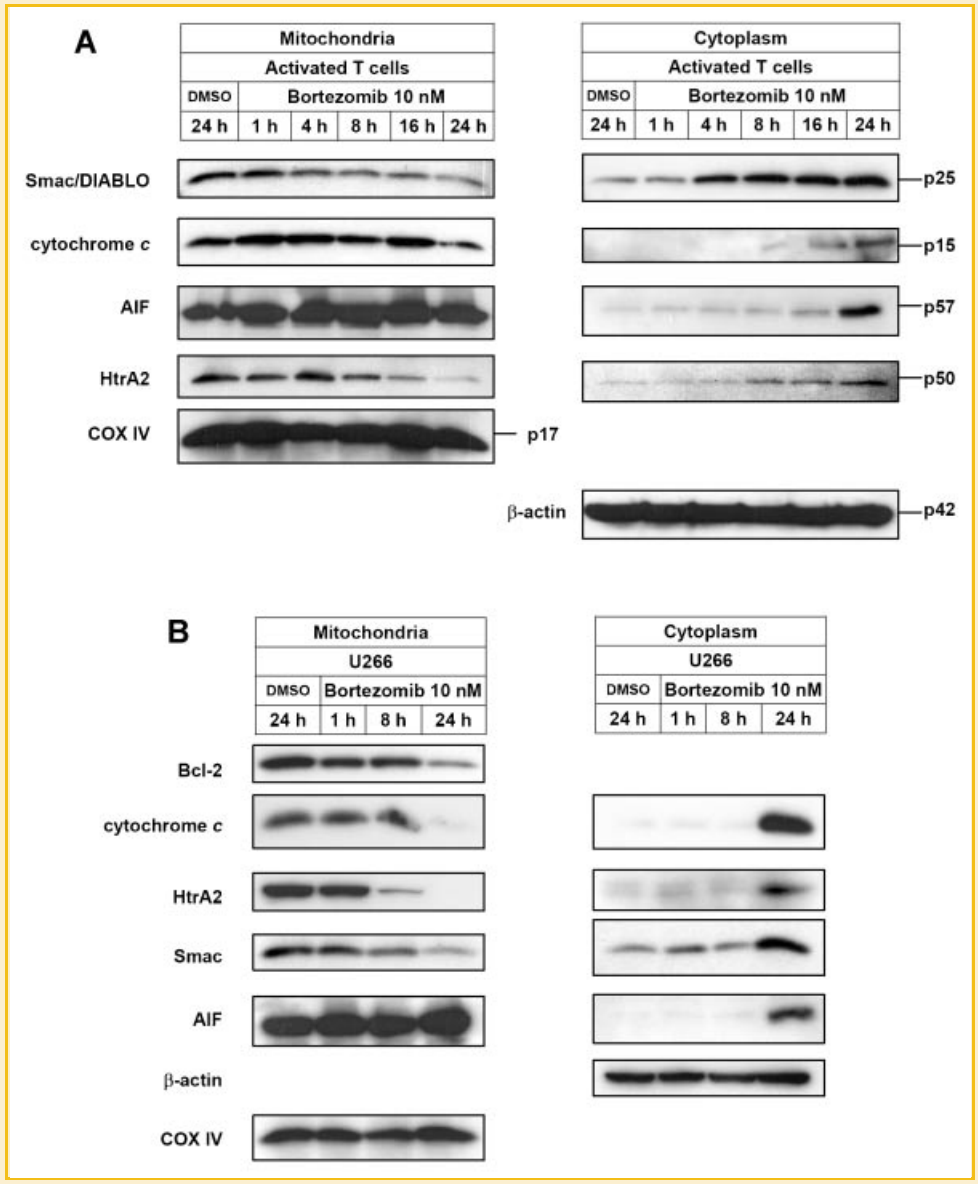

Fig. 5. Proteasome inhibition induces release of apoptogenic mitochondrial proteins into the cytoplasm. Subcellular fractions of activated $CD4^+$ T cells (A) and U266 B cells (B) were prepared and analyzed for the presence of Smac/DIABLO, cytochrome c, AIF, HtrA2 and Bcl-2 by immunoblot. Amounts of marker proteins for cytoplasmic and mitochondrial proteins β-actin and COX IV, respectively, are shown as a control of equal protein loading. Immunoblots were performed in triplicate with similar results.

REQUIREMENT FOR ROS GENERATION IN APOPTOSIS INDUCED BY PROTEASOME INHIBITION

To further investigate the role of ROS generation in apoptosis induced by proteasome inhibition, we determined ROS production and the extent of apoptosis in cells exposed for 24 h to bortezomib. Proteasome inhibition enhanced intracellular hydrogen peroxide levels in activated $CD4^+$ T cells, which could be blunted by preincubation with NAC (Fig. 6G; top panel). In addition, NAC significantly decreased apoptosis (Fig. 6D). In contrast, the specific pan-caspase inhibitor ZVAD displayed only a marginal effect on hydrogen peroxide generation induced by proteasome inhibition in activated $CD4^+$ T cells, but inhibited apoptosis in activated $CD4^+$ T cells as well as in U266 B cells to a greater extent than NAC. We also observed an increased induction of apoptosis by proteasome inhibition in U266 B cells as compared to activated $CD4^+$ T cells (Fig. 6E,F). These results indicate that proteasome inhibition triggers ROS generation that is independent of caspase activity in activated $CD4^+$ T cells, and amplifies apoptosis in activated $CD4^+$ T cells and U266 B cells.

DISCUSSION

The concept of proteasome inhibition in the treatment of several human neoplasias has been well established [Orlowski and Kuhn, 2008]. In addition, recent studies reveal that proteasome inhibition

leads to the attenuation of deregulated and unwanted T cell-mediated immune responses which contribute to the pathogenesis of autoimmune diseases, allograft rejection and GVHD [Luo et al., 2001; Sun et al., 2004; Mattingly et al., 2007; Everly et al., 2008; Neubert et al., 2008; Perry et al., 2008]. Studies performed by us and others strongly suggest that this suppressive effect of proteasome inhibition is achieved by inducing apoptosis selectively in activated T cells [Blanco et al., 2006; Berges et al., 2008], and to date the

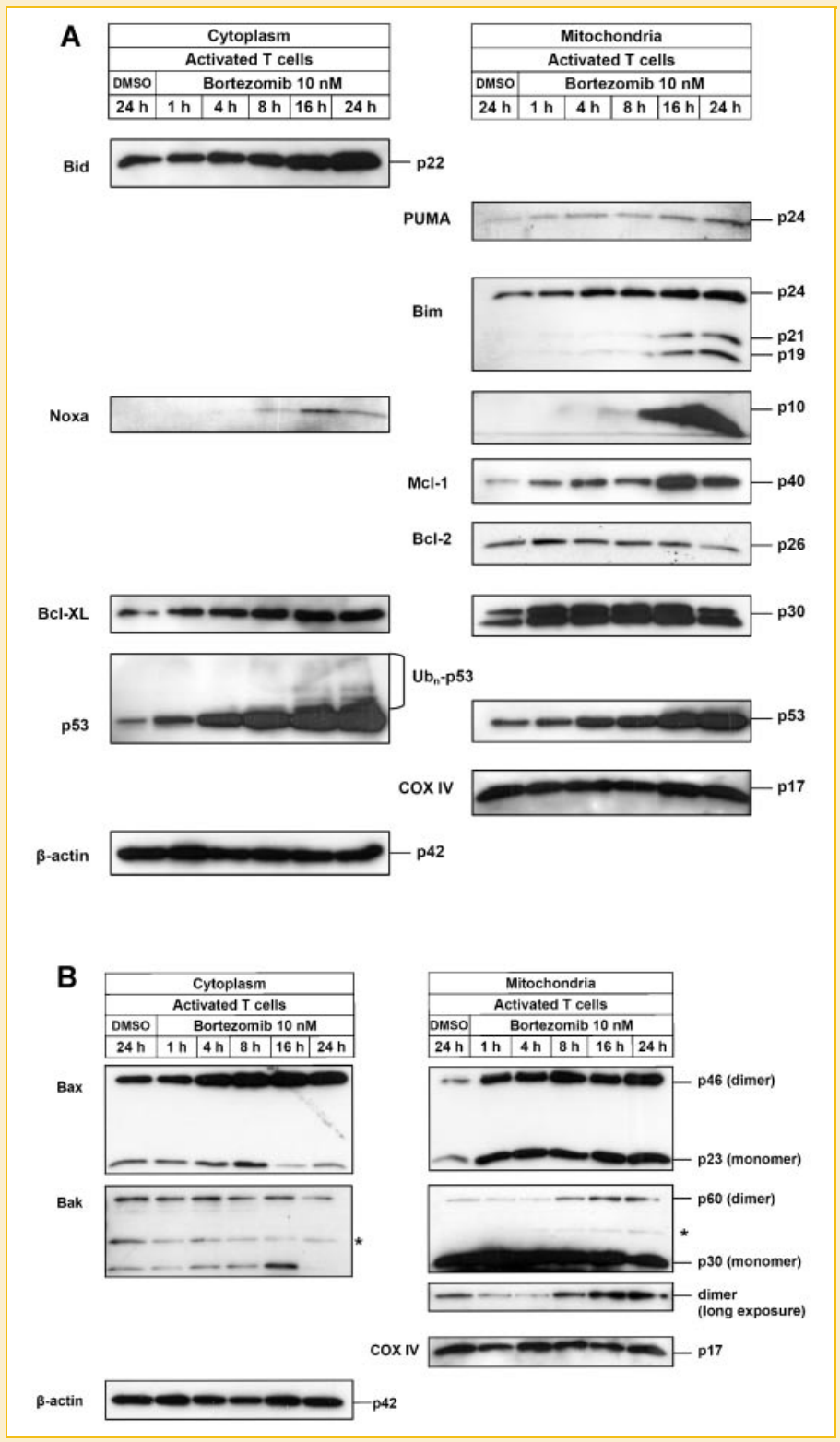

Fig. 6.

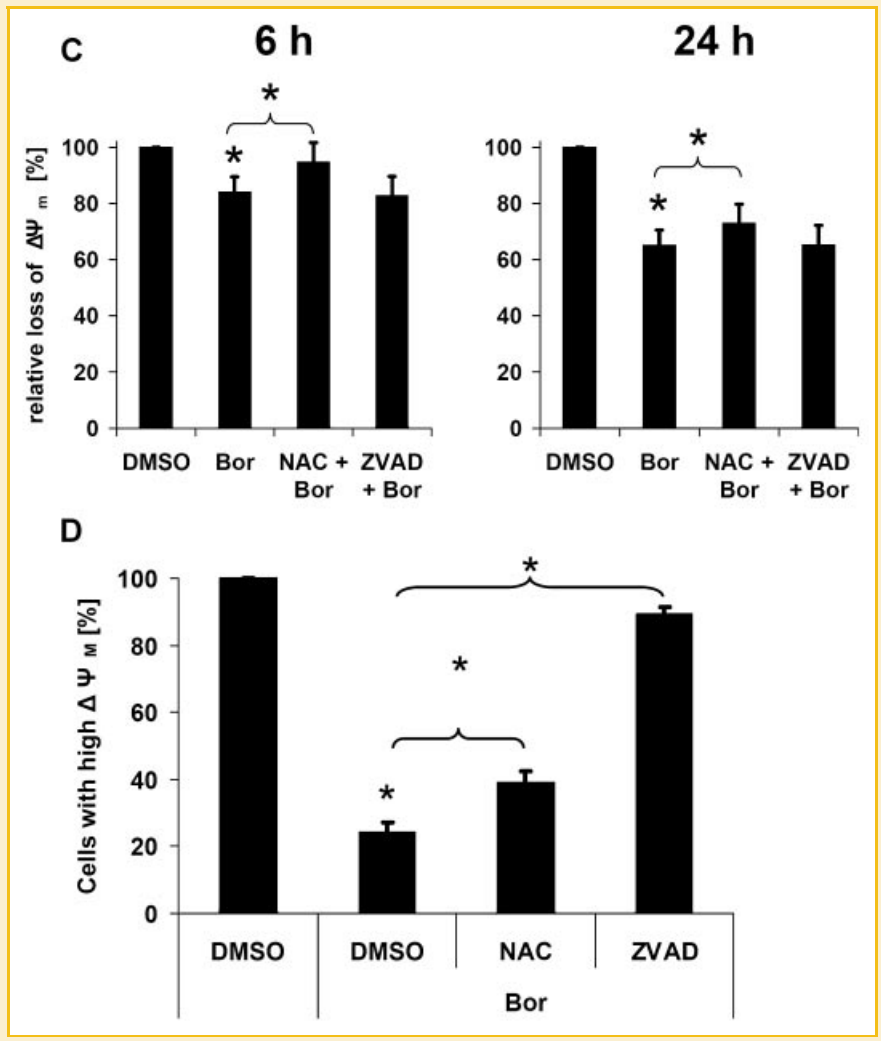

Fig. 6. (*Continued*)

apoptosis-inducing mechanisms of proteasome inhibition in T cells remain elusive.

Here we describe the mechanisms of apoptosis induced by proteasome inhibition in human $CD4^+$ T cells activated in a physiological manner by allogeneic DCs. In agreement with other reports [Misra et al., 2005; Lamkanfi et al., 2007], we found that activated $CD4^+$ T cells contain partially activated caspases, in particular caspase-3, -8, and -9.

Previous studies demonstrated that caspase activity under a non-apoptotic threshold is necessary for basic T cell functions, such as proliferation and differentiation [Misra et al., 2005; Lamkanfi et al., 2007]. Our results show that this intermediate caspase activity is tightly regulated by higher expression of c-FLIP, cIAP1, cIAP2 and XIAP in activated T cells compared to resting T cells [Vaux and Silke, 2005; Krammer et al., 2007]. We could also observe a predominant presence of caspase-3p20 and caspase-3p19, indicating that

Fig. 6. Proteasome inhibition triggers accumulation of apoptogenic proteins at the OMM, loss of $\Delta\Psi$m, apoptosis and ROS production. A,B: the same subcellular fractions as in Figure 5 were prepared and analyzed by immunoblot for the presence of A: Bid, PUMA, Bim, Noxa, Mcl-1, Bcl-2, Bcl-XL and p53 and B: Bax and Bak. Amounts of marker proteins for cytoplasmic and mitochondrial proteins, β-actin and COX IV, respectively, are shown as a control of equal protein loading. Immunoblots were performed in triplicate with similar results. Asterisks indicate non-specific bands. C: proteasome inhibition leads to loss of $\Delta\Psi$m. Naïve $CD4^+$ T cells were stimulated as described in Figure 1. Activated $CD4^+$ T cells (C) and U266 B cells (D) were pre-treated with 1 mM NAC, 100 μM ZVAD or DMSO for 1 h and subsequently exposed to DMSO or 10 nM Bor for 6 h (C) or 24 h (C,D), respectively. Thereafter, $\Delta\Psi$m were determined by flow cytometry as described in Materials and Methods Section. Data are given as mean values ± standard error of the mean of four independent experiments carried out in triplicate and are expressed relative to the loss of $\Delta\Psi$m with DMSO set to 100%. D: Pan-caspase inhibitor and ROS scavenger protects from apoptosis induced by proteasome inhibition. Activated $CD4^+$ T cells (E) and U266 B cells (F) were pre-treated with 1 mM NAC, 100 μM ZVAD or DMSO for 1 h and subsequently exposed to DMSO or 10 nM Bor for 24 h. Specific apoptosis was determined by flow cytometry as described in Materials and Methods Section. Data are given as mean values ± standard error of the mean of four independent experiments carried out in triplicate. $^*P < 0.05$. G, increases of intracellular hydrogen peroxide levels after proteasome inhibition. Activated $CD4^+$ T cells were pre-treated with 1 mM NAC, 100 μM ZVAD or DMSO for 1 h. Subsequently, cells were exposed to 10 nM Bor or DMSO for 6 h and stained with DCF followed by flow cytometry analysis. Data show one representative experiment out of four independent experiments.

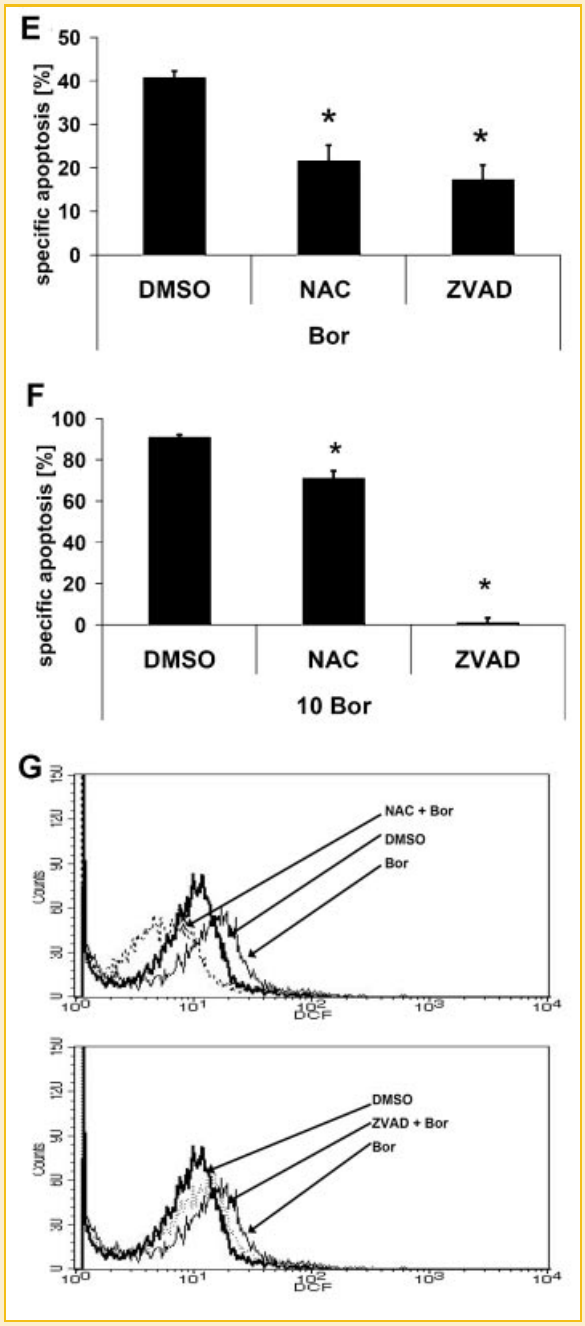

Fig. 6. (*Continued*)

pro-apoptotic caspase-3 activity is inhibited by direct interaction with XIAP [Sun et al., 2002]. Our results show that proteasome inhibition abrogates the tight regulation of caspases in activated T cells by triggering the mitochondrial pathway of apoptosis. We observed mitochondrial accumulation of pro-apoptotic Noxa, PUMA, Bim and of anti-apoptotic Mcl-1, whereas the anti-apoptotic Bcl-XL and Bcl-2 showed only a moderate or no mitochondrial accumulation. This effect can most probably attributed to proteasome inhibition-mediated accumulation of p53, which transcriptionally activates Noxa and PUMA and represses expression of Bcl-2 [Maki et al., 1996; Naujokat et al., 2000; Schuler and Green, 2001; Berges et al., 2008]. On the other hand, enrichment of all known Bim splice variants and of anti-apoptotic BH1-4 protein Mcl-1 at mitochondria is presumably a direct consequence of the inhibition of proteasomal degradation [Ley et al., 2003; Nencioni et al., 2005].

Besides its indirect role in transcriptional activation of pro-apoptotic proteins like Noxa, Puma and Bax, p53 has a direct apoptotic function at mitochondria [Schuler and Green, 2001]. Consistent with a previous study [Marchenko et al., 2007], we observed accumulation of monoubiquitinated and polyubiquitinated cytoplasmic and non-ubiquitinated mitochondrial p53. Our data suggest that activation of BH123 effector proteins Bax and Bak at the mitochondrial membrane in response to proteasome inhibition is most likely caused by a coordinated p53-induced mechanism which includes the synergistic cooperation of pro-apoptotic BH3-only proteins Bim, PUMA and Noxa as well as p53.

Upon activation by BH3-only proteins and p53, cytoplasmic Bax and mitochondrially localized Bak oligomerize into large complexes at the OMM, thereby disrupting the OMM integrity and inducing MOMP [Nechushtan et al., 1999; Wei et al., 2001]. We demonstrated that these proteasome inhibition-induced events cause breakdown of $\Delta\Psi m$ followed by cytoplasmic translocation of cytochrome *c*, Smac/DIABLO, HtrA2 and AIF. Interestingly, we observed that the release of Smac/DIABLO and HtrA2 precedes translocation of cytochrome *c* and AIF to the cytoplasm. These results are in accordance with studies postulating a different kinetic of release of intramitochondrial proteins into the cytoplasm. These studies suggest that different mechanisms govern the release of intramitochondrial proteins [Adrain et al., 2001; Uren et al., 2005]. It has been shown that generation of ROS amplifies MOMP and is necessary for the dissociation of cytochrome *c* and AIF from the mitochondrial inner membrane [Ott et al., 2002; Murahashi et al., 2003]. Nevertheless, we could not detect relevant ROS generation until 6 h after proteasome inhibition. In contrast, we could detect intermediate caspase activity, which is required for the rapid release of Smac/DIABLO into the cytoplasm after induction of MOMP [Adrain et al., 2001].

To extent our investigations to other cells of the hematopoietic lineage, we performed core experiments with U266 B cells. We demonstrate that bortezomib induces in these cells cytoplasmic translocation of pro-apoptotic Smac/DIABLO, cytochrome *c*, HtrA2 and AIF, as observed in activated T cells. Moreover, all intramitochondrial pro-apoptotic proteins analyzed exhibited equal kinetics of release from mitochondria in U266 B cells.

The rapid release of Smac/DIABLO and HtrA2 into the cytoplasm in response to proteasome inhibition leads to activation of caspases in response to abrogation of IAP inhibition. After proteasome inhibition we observed rapid further processing of caspase-3p20 to mature caspase-3p17 in activated $CD4^+$ T cells, obviously driven by the neutralization of XIAP-mediated inhibition of caspase-3. Moreover, some IAPs, like cIAP1, cIAP2 and XIAP, contain a RING-domain which enables them to act as an E3 ubiquitin ligase, thereby promoting ubiquitination and proteasomal degradation of themselves and of several of their binding partners, such as caspase-3, -9, and -7 [Sun et al., 2002; Vaux and Silke, 2005]. In this regard,

Smac/DIABLO has been shown not only to antagonize IAP-mediated inhibition of caspases, but also to enhance the intrinsic auto-ubiquitination activity of XIAP [Yang and Du, 2004]. Accordingly, we observed a time-dependent increase in ubiquitinated cIAP1 and XIAP. Proteasome inhibition most likely amplifies this effect by blocking the degradation of ubiquitinated IAPs. We suggest that proteasome inhibition induces an increase in abundance of IAP binding partners such as caspase-3, -9 and Smac/DIABLO [Vaux and Silke, 2005] and, thus, consolidate the already existing difference of the abundance of cytochrome *c* and Smac/DIABLO in the cytoplasm that is initiated by different kinetics of release in activated $CD4^+$ T cells. In addition, the intrinsic proteolytic activity of the serine protease HtrA2 that enables the degradation of IAPs serves as a further mechanism for neutralizing IAP-mediated caspase inhibition [Yang et al., 2003]. The decrease in cIAP1 and cIAP2 expression and the increase in XIAP cleavage products shown in our study may be traced back to HtrA2-mediated degradation. The concerted action of Smac/DIABLO and HtrA2 is likely to be responsible for the rapid augmentation of caspase-3 activity in activated $CD4^+$ T cells.

We found that increase in caspase-9 activity is followed by an enhancement of caspase-3 activity in activated $CD4^+$ T cells. This correlates with the delayed release of cytochrome *c* into the cytoplasm that is indispensable for activation of caspase-9 within the apoptosome. Consistent with a previous study, we therefore assume that Smac/DIABLO-activated caspase-3 initiates apoptosis induced by proteasome inhibition in activated T cells, whereas delayed activation of caspase-9 only accelerates apoptosis [Marsden et al., 2002]. In this case, caspase-3-mediated disruption of XIAP inhibition by cleavage of caspase-9 to caspase-9p37 abrogates caspase-9 activation [Denault et al., 2007]. A similar important role of Smac/DIABLO and effector caspases, such as caspase-3 in apoptosis induced by proteasome inhibition has been described by others [Henderson et al., 2005].

Since inhibition of caspase activity with ZVAD could not completely block apoptosis, we assume that proteasome inhibition activates a caspase-independent apoptotic pathway in T cells. In U266 B cells caspase inhibition nearly completely blocked apoptosis induced by bortezomib. Furthermore, ZVAD decreased $\Delta\Psi m$ breakdown, suggesting an important role for caspase activity in the initiation of mitochondrial apoptosis pathway in these cells. In the present study, we show that proteasome inhibition triggers translocation of AIF to the cytoplasm with a similar kinetic as cytochrome *c*. This event is presumably caspase-independent, but is regulated by ROS production in response to proteasome inhibition, as previously shown [Susin et al., 1999; Yu et al., 2003]. Accordingly, we observed a significant decrease of $\Delta\Psi m$ breakdown in response to proteasome inhibition after addition of NAC, demonstrating a critical role for ROS generation in apoptosis induced by proteasome inhibition in activated T cells and U266 B cells [Chauhan et al., 2005; Perez-Galan et al., 2006].

In summary, our data show that proteasome inhibition triggers the mitochondrial pathway of apoptosis in activated T cells by triggering caspase-dependent and caspase-independent apoptotic pathways. Our study also implicates that the mechanisms of apoptosis induced by the proteasome inhibitor bortezomib need further investigation in order to identify possible unwanted side effects of bortezomib therapy. We could elucidate the mechanism of apoptosis following proteasome inhibition in activated T cells and thus provide an experimental basis for a future use of proteasome inhibitors as immunosuppressive agents.

ACKNOWLEDGMENTS

The excellent technical assistance of Marion Miltz-Savidis, Regina Seemuth, and Martina Kutsche-Bauer is gratefully acknowledged.

REFERENCES

Adrain C, Creagh EM, Martin SJ. 2001. Apoptosis-associated release of Smac/DIABLO from mitochondria requires active caspases and is blocked by Bcl-2. EMBO J 20:6627–6636.

Berger AB, Sexton KB, Bogyo M. 2006. Commonly used caspase inhibitors designed based on substrate specificity profiles lack selectivity. Cell Res 16: 961–963.

Berges C, Haberstock H, Fuchs D, Miltz M, Sadeghi M, Opelz G, Daniel V, Naujokat C. 2008. Proteasome inhibition suppresses essential immune functions of human CD4+ T cells. Immunology 124:234–246.

Blanco B, Pérez-Simón JA, Sánchez-Abarca LI, Carvajal-Vergara X, Mateos J, Vidriales B, López-Holgado N, Maiso P, Alberca M, Villarón E, Schenkein D, Pandiella A, San Miguel J. 2006. Bortezomib induces selective depletion of alloreactive T lymphocytes and decreases the production of Th1 cytokines. Blood 107:3575–3583.

Chauhan D, Hideshima T, Anderson KC. 2005. Proteasome inhibition in multiple myeloma: Therapeutic implication. Annu Rev Pharmacol Toxicol 45:465–476.

Ciechanover A. 2006. The ubiquitin proteolytic system. Neurology 66(Suppl 1):S7–S19.

Denault JB, Eckelman BP, Shin H, Pop C, Salvesen GS. 2007. Caspase 3 attenuates XIAP (X-linked inhibitor of apoptosis protein)-mediated inhibition of caspase 9. Biochem J 405:11–19.

Dhein J, Walczak H, Bäumler C, Debatin KM, Krammer PH. 1997. Autocrine T-cell suicide mediated by APO-1/(Fas/CD95). Nature 373:438–441.

Drexler HCA. 1997. Activation of the cell death program by inhibition of proteasome function. Proc Natl Acad Sci USA 94:855–860.

Everly MJ, Everly JJ, Susskind B, Brailey P, Arend LJ, Alloway RR, Roy-Chaudhury P, Govil A, Mogilishetty G, Rike AH, Cardi M, Wadih G, Tevar A, Woodle ES. 2008. Bortezomib provides effective therapy for antibody- and cell-mediated acute rejection. Transplantation 86:1754–1761.

Fuchs D, Berges C, Opelz G, Daniel V, Naujokat C. 2008a. Increased expression and altered subunit composition of proteasomes induced by continuous proteasome inhibition establish apoptosis resistance and hyperproliferation of Burkitt lymphoma cells. J Cell Biochem 103:270–283.

Fuchs D, Berges C, Opelz G, Daniel V, Naujokat C. 2008b. HMG-CoA reductase inhibitor simvastatin overcomes bortezomib-induced apoptosis resistance by disrupting a geranylgeranyl pyrophosphate-dependent survival pathway. Biochem Biophys Res Commun 374:309–314.

Glickman MH, Ciechanover A. 2002. The ubiquitin-proteasome proteolytic pathway: Destruction for the sake of construction. Physiol Rev 82:373–428.

Goping IS, Gross A, Lavoie JN, Nguyen M, Jemmerson R, Roth K, Korsmeyer SJ, Shore GC. 1998. Regulated targeting of Bax to mitochondria. J Cell Biol 143:207–215.

Groll M, Huber R. 2004. Inhibitors of the eukaryotic 20S proteasome core particle: A structural approach. Biochim. Biophys Acta 1695:33–44.

Henderson CJ, Aleo E, Fontanini A, Maestro R, Paroni G, Brancolini C. 2005. Caspase activation and apoptosis in response to proteasome inhibitors. Cell Death Differ 12:1240–1254.

Karst AM, Li G. 2007. BH3-only proteins in tumorigenesis and malignant melanoma. Cell Mol Life Sci 64:318–330.

Krammer PH, Arnold R, Lavrik IN. 2007. Life and death in peripheral T cells. Nat Rev Immunol 7:532–542.

Lamkanfi M, Festjens N, Declercq W, Vanden Berghe T, Vandenabeele P. 2007. Caspases in cell survival, proliferation and differentiation. Cell Death Differ 14:44–55.

Ley R, Balmanno K, Hadfield K, Weston C, Cook SJ. 2003. Activation of the ERK1/2 signaling pathway promotes phosphorylation and proteasome-dependent degradation of the BH3-only protein, Bim. J Biol Chem 278: 18811–18816.

Luo H, Wu Y, Qi S, Wan X, Chen H, Wu J. 2001. A proteasome inhibitor prevents mouse heart allograft rejection. Transplantation 72:196–202.

Maki CG, Huibregtse M, Howley PM. 1996. In vivo ubiquitination and proteasome-mediated degradadtion of p53. Cancer Res 56:2649–2654.

Marchenko ND, Wolff S, Erster S, Becker K, Moll UM. 2007. Monoubiquitylation promotes mitochondrial p53 translocation. EMBO J 26:923–934.

Marsden VS, O'Connor L, O'Reilly LA, Silke J, Metcalf D, Ekert PG, Huang DC, Cecconi F, Kuida K, Tomaselli KJ, Roy S, Nicholson DW, Vaux DL, Bouillet P, Adams JM, Strasser A. 2002. Apoptosis initiated by Bcl-2-regulated caspase activation independently of the cytochrome c/Apaf-1/caspase-9 apoptosome. Nature 419:634–637.

Mattingly LH, Gault RA, Murphy WJ. 2007. Use of systemic proteasome inhibition as an immune-modulating agent in disease. Endocr Metab Immune Disord Drug Targets 7:29–34.

Miller CP, Ban K, Dujka ME, McConkey DJ, Munsell M, Palladino M, Chandra J. 2007. NPI-0052, a novel proteasome inhibitor, induces caspase-8 and ROS-dependent apoptosis alone and in combination with HDAC inhibitors in leukemia cells. Blood 110:267–277.

Misra RS, Jelley-Gibbs DM, Russell JQ, Huston G, Swain SL, Budd RC. 2005. Effector $CD4^+$ T cells generate intermediate caspase activity and cleavage of caspase-8 substrates. J Immunol 174:3999–4009.

Murahashi H, Azuma H, Zamzami N, Furuya KJ, Ikebuchi K, Yamaguchi M, Yamada Y, Sato N, Fujihara M, Kroemer G, Ikeda H. 2003. Possible contribution of apoptosis-inducing factor (AIF) and reactive oxygen species (ROS) to UVB-induced caspase-independent cell death in the T cell line Jurkat. J Leukoc Biol 73:399–406.

Naujokat C, Hoffmann S. 2002. Role and function of the 26S proteasome in proliferation and apoptosis. Lab Invest 82:965–980.

Naujokat C, Sezer O, Zinke H, Leclere A, Hauptmann S, Possinger K. 2000. Proteasome inhibitors induce caspase-dependent apoptosis and accumulation of p21 in human immature leukemic cells. Eur J Haematol 65:221–236.

Naujokat C, Berges C, Höh A, Wieczorek H, Fuchs D, Ovens J, Sadeghi M, Opelz G, Daniel V. 2007a. Proteasomal chymotrypsin-like peptidase activity is required for essential functions of human monocyte-derived dendritic cells. Immunology 120:20–32.

Naujokat C, Fuchs D, Berges C. 2007b. Adaptive modification and flexibility of the proteasome system in response to proteasome inhibition. Biochim Biophys Acta 1773:1389–1397.

Nechushtan A, Smith CL, Hsu YT, Youle RJ. 1999. Conformation of the Bax C-terminus regulates subcellular location and cell death. EMBO J 18:2330–2341.

Nencioni A, Hua F, Dillon CP, Yokoo R, Scheiermann C, Cardone MH, Barbieri E, Roccom I, Garuti A, Wesselborg S, Belka C, Brossart P, Patrone F, Ballestrero A. 2005. Evidence for a protective role of Mcl-1 in proteasome inhibitor-induced apoptosis. Blood 105:3255–3262.

Neubert K, Meister S, Moser K, Weisel F, Maseda D, Amann K, Wiethe C, Winkler TH, Kalden JR, Manz RA, Voll RE. 2008. The proteasome inhibitor bortezomib depletes plasma cells and protects mice with lupus-like disease from nephritis. Nat Med 14:748–755.

Orlowski RZ, Kuhn DJ. 2008. Proteasome inhibitors in cancer therapy: Lessons from the first decade. Clin Cancer Res 14:1649–1657.

Ott M, Robertson JD, Gogvadze V, Zhivotovsky B, Orrenius S. 2002. Cytochrome c release from mitochondria proceeds by a two-step process. Proc Natl Acad Sci USA 99:1259–1263.

Perez-Galan P, Roue G, Villamor N, Montserrat E, Campo E, Colomer D. 2006. Cytochrome c release from mitochondria proceeds by a two-step process. Blood 107:257–264.

Perry DK, Burns JM, Pollinger HS, Amiot BP, Gloor JM, Gores GJ, Stegall MD. 2008. Proteasome inhibition causes apoptosis of normal human plasma cells preventing alloantibody production. Am J Transplant 8:1–9.

Schuler M, Green DR. 2001. Mechanisms of p53-dependent apoptosis. Biochem Soc Trans 29:684–688.

Sun XM, Bratton SB, Butterworth M, Mac Farlane M, Cohen GM. 2002. Bcl-2 and Bcl-xL inhibit CD95-mediated apoptosis by preventing mitochondrial release of Smac/DIABLO and subsequent inactivation of X-linked inhibitor-of-apoptosis protein. J Biol Chem 277:11345–11351.

Sun K, Welniak LA, Panoskaltsis-Mortari A, O'Shaughnessy MJ, Liu H, Barao I, Riordan W, Sitcheran R, Wysocki C, Serody JS, Blazar BR, Sayers TJ, Murphy WJ. 2004. Inhibition of acute graft-versus-host disease with retention of graft-versus-tumor effects by the proteasome inhibitor bortezomib. Proc Natl Acad Sci USA 101:8120–8125.

Susin SA, Lorenzo HK, Zamzami N, Marzo I, Snow BE, Brothers GM, Mangion J, Jacotot E, Costantini P, Loeffler M, Larochette N, Goodlett DR, Aebersold R, Siderovski DP, Penninger JM, Kroemer G. 1999. Molecular characterization of mitochondrial apoptosis-inducing factor. Nature 397:441–446.

Uren RT, Dewson G, Bonzon C, Lithgow T, Newmeyer DD, Kluck RM. 2005. Mitochondrial release of pro-apoptotic proteins: Electrostatic interactions can hold cytochrome c but not Smac/DIABLO to mitochondrial membranes. J Biol Chem 280:2266–2274.

Vaux DL, Silke J. 2005. IAPs, RINGs and ubiquitylation. Nat Rev Mol Cell Biol 6:2872–2897.

Wei MC, Zong WX, Cheng EH, Lindsten T, Panoutsakopoulou V, Ross AJ, Roth KA, MacGregor GR, Thompson CB, Korsmeyer SJ. 2001. Proapoptotic BAX and BAK: A requisite gateway to mitochondrial dysfunction and death. Science 292:727–730.

Yang QH, Du C. 2004. Smac/DIABLO selectively reduces the levels of c-IAP1 and c-IAP2 but not that of XIAP and livin in HeLA cells. J Biol Chem 279: 16963–16970.

Yang QH, Church-Hajduk R, Ren J, Newton ML, Du C. 2003. Omi/HtrA2 catalytic cleavage of inhibitor of apoptosis (IAP) irreversibly inactivates IAPs and facilitates caspase activity in apoptosis. Genes Dev 17:1487–1496.

Yu C, Rahmani M, Conrad D, Subler M, Dent P, Grant S. 2003. The proteasome inhibitor bortezomib interacts synergistically with histone deacetylase inhibitors to induce apoptosis in Bcr/Abl + cells sensitive and resistant to STI571. Blood 102:3765–3774.